

# Giant piezoresistivity of polymer-derived ceramics at high temperatures<sup>☆</sup>

K. Terauds<sup>a</sup>, P.E. Sanchez-Jimenez<sup>a</sup>, R. Raj<sup>a,\*</sup>, C. Vakifahmetoglu<sup>b</sup>, P. Colombo<sup>b,c</sup>

<sup>a</sup> Department of Mechanical Engineering, Engineering Center - ECME 114, University of Colorado at Boulder, Boulder, CO 80309-0427, United States

<sup>b</sup> Dipartimento di Ingegneria Meccanica - Settore Materiali, Università di Padova, via Marzolo, 9, 35131 Padova, Italy

<sup>c</sup> Department of Materials Science and Engineering, The Pennsylvania State University, University Park, PA 16802, United States

Available online 25 March 2010

## Abstract

The piezoresistivity of a silicon oxycarbonitride polymer-derived ceramic (PDC) material is investigated at high temperatures. The resistance was measured as a function of uniaxial loading under constant current conditions. The piezoresistive gage factor was found to be in the range of 600–1700 at an applied stress of 1 MPa. The gage factor depends on both the stress and temperature. The piezoresistivity was measured up to 1000 °C, demonstrating the viability of PDCs as piezoresistive materials at high temperatures. The Arrhenius dependence of the gage factor,  $\psi$ , gives the following expression for its temperature dependence at 1 MPa:  $\psi = 44 \exp(28,000/8.31T)$ , where  $T$  is in Kelvin. The extrapolated values of the gage factor yield a value of 322 at 1400 °C, and 287 at 1500 °C (at an applied stress of 1 MPa). A combination of stability at high temperatures, chemical durability, and large gage factor are entirely unique to PDCs making them ideal candidates for sensor materials in extreme environments. © 2010 Elsevier Ltd. All rights reserved.

**Keywords:** Polymer-derived ceramic; Electrical properties; Electrical conductivity; Mechanical properties; Sensors

## 1. Introduction

Polymer-derived-ceramics (PDCs) are a new class of materials produced from the decomposition of organic polymer precursors. The PDCs offer a unique combination of properties akin to both polymers and ceramics. The unusual attributes of PDCs stem from their amorphous nanodomain structure. The structure consists of an organic graphene network with typical domain sizes in the range of 1–5 nm.<sup>1,2</sup> Special properties of PDCs include high oxidation and thermal shock resistance, and zero creep behavior, which make them a distinctive class of high temperature ceramics.<sup>3–5</sup> It has been shown that PDCs remain stable up to 1400–1500 °C and, in special cases, even at 2000 °C.<sup>6</sup> The PDCs have been shown to hold promise for high temperature membranes, oxidation resistant coatings, and flux sensors for gas turbine engines.<sup>7–9</sup>

In addition to their structural properties and chemical stability, the PDCs also possess functional properties of different

kinds. They are semiconductors at least up to 1300 °C.<sup>10</sup> Though amorphous, they are intensely photoluminescent<sup>11</sup> with a wide spectrum emission. Recently they were shown to have giant gage factors for piezoresistivity at room temperature.<sup>12,13</sup> Such functional properties of the PDCs are sensitive to their composition and processing and, therefore, it would be possible to tailor them for specific applications.

The PDCs are also attractive for multifunctional applications because they are processed from the polymer route at low temperatures (in this respect they are unusual since conventional ceramics must be processed at a temperature that is higher than their service temperature). The polymer route to processing enables photolithographic methods for fabrication of MEMS-scale sensor devices, employing commonly used techniques for photoresists in the electronics industry.<sup>14–17</sup>

Today's most common piezoresistive sensor materials are doped silicon and germanium. The elevated temperature performance of these materials is typically limited to below 200 °C. Newer materials, such as diamond films and SiC, possess better operating ranges but are still limited to relatively low temperatures.

The purpose of this paper is to characterize the piezoresistivity of a polymer-derived SiCNO at elevated temperatures up to 1000 °C. The results yield very large values for the piezoresistive gage factor, raising the specter of a new class of high temperature stress and strain sensors.

<sup>☆</sup> This paper was presented at the Air Force Office of Scientific Research (AFOSR) Workshop on Aerospace Materials for Extreme Environments, held August 3–5, 2009 in St. Louis, MI.

\* Corresponding author. Tel.: +1 303 492 1029; fax: +1 303 492 3498.  
E-mail address: [rishi.raj@colorado.edu](mailto:rishi.raj@colorado.edu) (R. Raj).

## 2. Methods/experimental procedure

### 2.1. Sample preparation

The samples were prepared in two steps. In step one, a *silicon oxycarbide* specimen was prepared using the process described just below. These specimens were non-conducting. In step two, nitrogen was exchanged with oxygen to render them electrically conducting, using the high pressure nitrogen annealing process at high temperatures.<sup>10</sup> Even minor exchange of oxygen with nitrogen, here by a mere 6% atom fraction makes the specimens electronically conducting.

In step one, the samples were prepared using a commercially available preceramic polymer, poly(methyl)silsesquioxane (MK, Wacker Chemie AG, Burghausen, Germany; denoted as PMS). 7 g of PMS precursor was thermally cross-linked at 250 °C for 5 h in air, and 3 g of PMS precursor was partially cross-linked at 100 °C for 15 min in air to act as a binder (for both of the curing process heating and cooling rate was set to 2 °C/min). Then both powders were mixed together and ball milled at 350 rpm. The powder was then cold pressed in a steel die at 15 MPa.

The powder pressed greenbody was pyrolyzed at 1200 °C in a furnace with tungsten elements under a nitrogen atmosphere. The cycle was ramped to 1200 °C at 2 °C/min, held for 2 h, and then cooled to room temperature at 2 °C/min. The sample remains an electrical insulator after the pyrolysis. In step two, the sample was rendered to be conductive by heat treating for 45 h in a hot-isostatic-press (HIP) under nitrogen atmosphere with a peak temperature of 1400 °C and a maximum pressure of 26.2 MPa. The pyrolysis and HIP cycles are shown in Fig. 1. After heat treatment, the sample was 3.0 mm thick with a 3.4 mm × 4.2 mm cross-section and had a room temperature conductivity of  $2.0 \times 10^{-4} \Omega^{-1} \text{cm}^{-1}$ .

The chemical composition of the sample was measured using a LECO C-200 Carbon Analyzer and a LECO TC-600 Oxygen-Nitrogen Determinator. The carbon, nitrogen, and oxygen compositions by weight were measured to be  $10.6 \pm 0.3\%$ ,  $2.55 \pm 0.06\%$  and  $40.21 \pm 1.8\%$ , respectively; the balance,

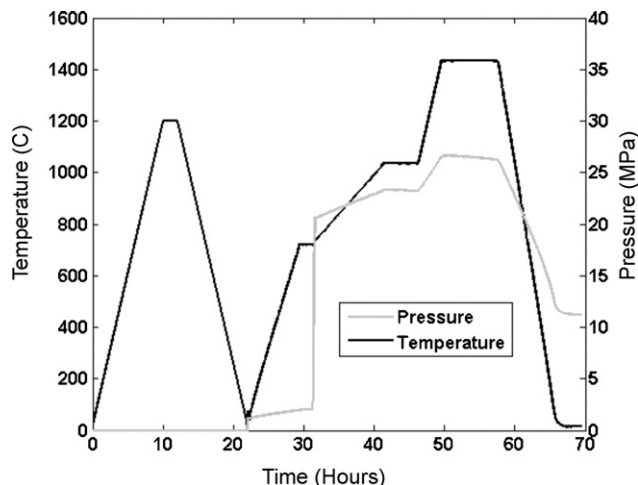


Fig. 1. Pyrolysis and heat treatment schedule.

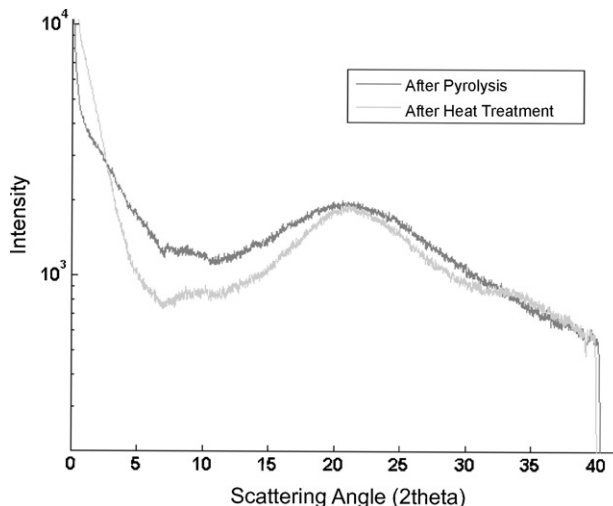


Fig. 2. Absence of diffraction X-ray peaks indicating amorphous structure.

46.64%, was assumed to be the weight fraction of silicon. These measurements gave the following molar composition for the sample:  $\text{Si}_{0.32}\text{C}_{0.17}\text{N}_{0.03}\text{O}_{0.48}$ . The room temperature conductivity of the sample was an order of magnitude lower than measured in Ref. 10. Although the nitrogen to oxygen ratio in both studies was similar, the silicon to carbon ratio in the present experiments was higher than in Ref. 10, which may have been responsible for the lower conductivity.

The X-ray diffraction of the samples, after pyrolysis, and then again after the heat treatment in the hot-isostatic-press are shown in Fig. 2. They confirm the amorphous nature of the samples.

### 2.2. Electrical measurements under applied stress at high temperature

The experimental set-up for the stress-dependent electrical measurements is described in Fig. 3. The sample was heated from 700 °C to 1000 °C in an Applied Test Systems cylindrical furnace. Temperature was measured with a K-type thermocouple positioned next to the sample. The sample was loaded in uniaxial compression by an Enterpac 10-ton hydraulic press using alumina rods as extensions. The force was measured by a Strain-Sert universal load cell. Pliable graphite paper with nickel lead wires was used between the alumina rods and SiCNO sample as electrodes. The sample was immersed in a flowing Argon atmosphere to prevent oxidation of the graphite electrodes. A constant current of 3.15 mA was applied across the sample using a Sorensen 300-2 power supply. The voltage change between electrodes was measured using a Keithley 2000 Multimeter. Sample resistance was then calculated from the known current and measured voltage using Ohm's law. The validity of the Ohm's law was ascertained. Fig. 4 shows the linear voltage–current relationship across the sample at a fixed temperature and stress. (A linear least-squares fit to the  $V$ – $I$  data set gave an  $R$ -squared value of 0.9998.)

The piezoresistive measurements were made by raising the furnace to the test temperature and holding at that temperature for 15 min. Compressive loads ranging from zero to 10 MPa

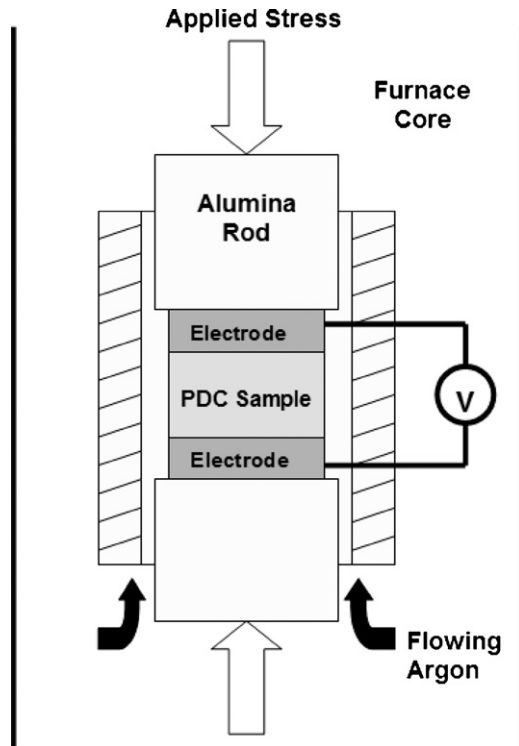


Fig. 3. Schematic of experimental setup.

were then applied in several cycles of loading and unloading. The effect of the applied stress on the resistance of the specimen was reproducible. The loading and unloading cycles gave the same result for the stress dependence of resistance, confirming reversible elastic (and piezoresistive) behavior.

### 3. Results

The stress–resistance curves, measured at 700 °C, 800 °C, 900 °C and 1000 °C are shown in Fig. 5. In each case a sharp change in resistance is seen when the specimen is loaded; this drop is ascribed to a change in the contact resistance between

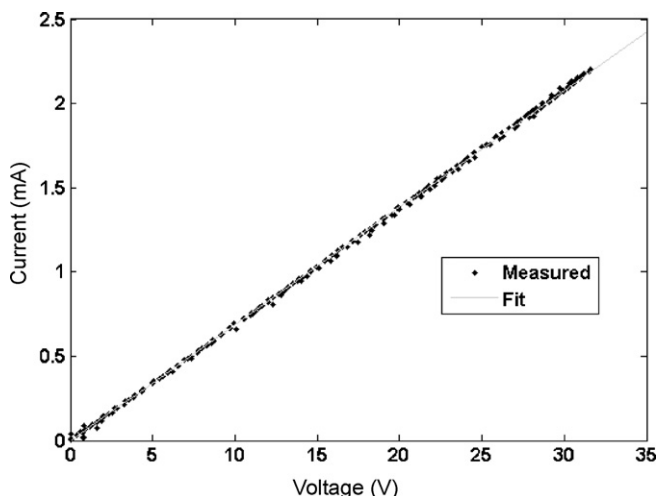


Fig. 4. Linear voltage–current behavior.

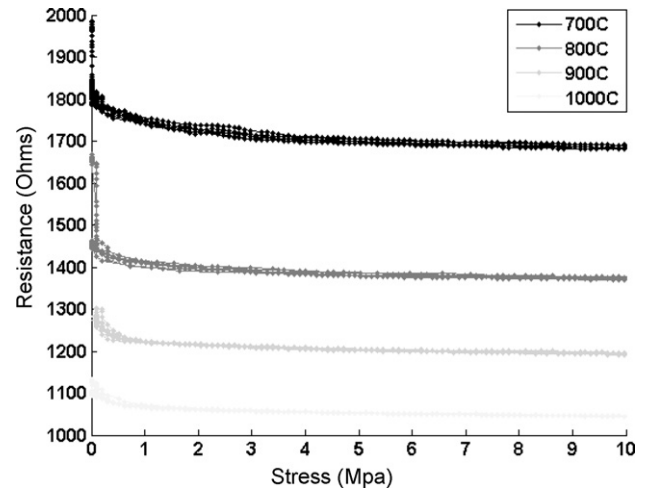


Fig. 5. Resistance load cycles up to 1000 °C.

the graphite electrodes and the sample since the graphite was in the form of a flexible foil which would need to be pressed closely against the sample face to achieve good electrical contact. These early points (below 0.5 MPa) have been omitted in the subsequent analysis.

The gage factor,  $K$ , was calculated by

$$K = \frac{1}{R} \cdot \frac{dR}{d\varepsilon} \quad (1)$$

where  $R$  is the sample resistance and  $\varepsilon$  is the applied elastic strain. The strain was calculated from the applied stress using a Young's modulus of 97 GPa, the value measured by Cross and Raj<sup>18</sup> on a sample with a similar composition ( $\text{SiC}_{0.50}\text{N}_{0.03}\text{O}_{0.47}$ ). The slope,  $dR/d\varepsilon$ , was calculated from a nonlinear least-squares fit to the stress–resistance curves in the form of

$$R = c_1 + c_2 \cdot e^{-\sigma/c_3} \quad (2)$$

where  $c_1$ ,  $c_2$ , and  $c_3$  are numerical constants, and  $\sigma$  is the applied stress. A chi-squared goodness of fit hypothesis test was performed on each curve verifying that all non-random variance in the data was explained by Eq. (2).

The results for the piezoresistivity gage factor are given in Fig. 6. The gage factor varies within the range 600–1700 near an applied stress of 1 MPa. However, it varies strongly with stress and temperature. A decreasing gage factor with higher stress is in agreement with the room temperature piezoresistivity of PDCs reported by An and coworkers.<sup>12</sup> The high temperature piezoresistive gage factors of various materials, including the present, are compared in Table 1.<sup>19–25</sup>

Table 1

A comparison of the gage factor of PDC (SiCNO) with other piezoresistive materials at ambient and higher temperature.

Material	Gage factor	Temperature limit (°C)
Germanium	10	135
Silicon	180	200
SiCNO	~1000	>1000
Diamond	100	300
Silicon carbide	40	500

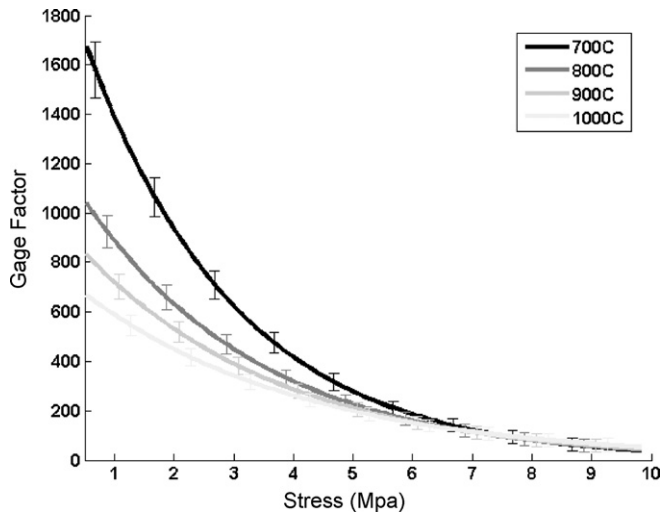


Fig. 6. Stress dependent gage factor up to 1000 °C.

#### 4. Discussion

The underlying molecular mechanism for the large piezoresistivity gage factors in PDCs remains an open question. However, some insights can be gained by calculating the activation energies for the temperature dependence of both the resistivity and the gage factors in the present study.

The PDCs are amorphous structures which are expected to contain nanodomain networks of graphene, and mixed bonds of silicon, carbon, oxygen and nitrogen. The electronic properties of these SiCNO based ceramics depend greatly on their composition. For example, the conductivity can change by up to six orders of magnitude by changing the N to O ratio.<sup>10</sup> The semi-conducting properties of these PDCs have been explained principally by the variable range hopping (VRH) mechanism.<sup>10</sup> In this mechanism the mobility of the charge carriers is related to a hopping distance, which is often much larger than the nearest neighbor distance in the molecular network, and by a hopping energy. The hopping energy is usually in the few tenths of eV range.

Arrhenius plots of the resistance and the gage factors from the present experiments are given in Fig. 7. The resistance has an activation energy of 0.17 eV, which is typical of the hop-

ping energy that was measured for the VRH mechanism.<sup>10</sup> Interestingly the activation energy for the gage factor, which is reasonably consistent at three levels of the applied stress, is larger by a factor of two. The data are not extensive enough to draw an inference as to whether the effect of the applied elastic strain is to alter the hopping distance or the hopping energy. At first glance it would appear that the applied elastic strain has a significant influence on the hopping distance since the activation energy for the gage factor is greater than the activation energy for the baseline resistance.

A fit of the gage factor to the Arrhenius plot given in Fig. 7, gives the following expression for the gage factor,  $\psi$ , at a stress of 1 MPa:

$$\psi = 44 \exp\left(\frac{28,000}{8.31T}\right) \quad (3)$$

Here  $T$  the temperature is expressed in K. Extrapolating Eq. (3) to 1400 °C gives a value of 322 for the gage factor. At 1500 °C, a value of 287 is predicted. These values are large in themselves. That they may hold at ultrahigh temperatures is all the more remarkable.

#### 5. Summary

The piezoresistive properties of a polymer-derived ceramic having the composition,  $\text{Si}_{0.32}\text{C}_{0.17}\text{N}_{0.03}\text{O}_{0.48}$ , was measured in the temperature range of 700–1000 °C at stresses ranging from 1 MPa to 10 MPa. The gage factor is strongly stress and temperature dependent. In this full range of stress and temperature the gage factor varies between 100 and 1700, with the lowest value relating to the highest stress and temperature, and the highest value to the lowest stress and temperature. The piezoresistive behavior of the PDCs far exceeds the performance of any known materials in this temperature range.

#### Acknowledgements

This research was supported by Dr. Joan Fuller at the Air Force Office of Scientific Research under Grant No. FA9550-09-1-005, and by the Ceramics Program of the Division of Materials Research at the National Science Foundation under Grant No.: 0502781.

#### References

1. Resta N, Kohler C, Trebin HR. Molecular dynamics simulations of amorphous SiCN ceramics: composition dependence of the atomic structure. *J Am Ceram Soc* 2003;**86**(8):1409–14.
2. Saha A, Williamson DL, Raj R. A model for nanodomains in polymer-derived SiCO. *J Am Ceram Soc* 2006;**89**(7):2188–95.
3. Raj R, An L, Shah S, Riedel R, Fasel C, Kleebe HJ. Oxidation kinetics of amorphous silicon carbonitride ceramics. *J Am Ceram Soc* 2001;**84**(8):1805–10.
4. Raj R, Riedel R, Soraru GD. Introduction to the special topical issue on ultrahigh-temperature polymer-derived ceramics. *J Am Ceram Soc* 2001;**84**(10):2158–9.
5. An L, Riedel R, Konetschny C, Kleebe HJ, Raj R. Newtonian viscosity of amorphous silicon carbonitride at high temperature. *J Am Ceram Soc* 1998;**81**(5):1349–52.

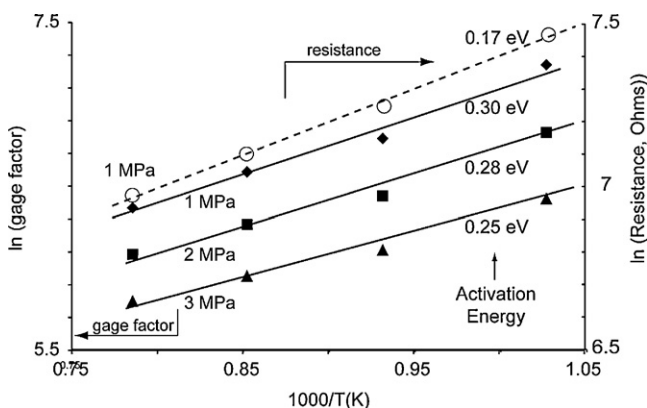


Fig. 7. An Arrhenius plot of the gage factor (solid lines) at different values of the applied stress, and the resistance (dashed line).

6. Riedel R, Kienzle A, Dressler W, Ruwisch L, Bill J, Aldinger F. A sili-coboron carbonitride ceramic stable to 2000 °C. *Nature* 1996;**382**(August (6594)):796–8.
7. Hauser R, Nahar-Borchard S, Riedel R, Ikuhara YH, Iwamoto Y. Polymer-derived SiBCN ceramic and their potential application for high temperature membranes. *J Ceram Soc Jpn* 2006;**114**(June (6)):524–8.
8. Torrey JD, Bordia RK. Mechanical properties of polymer-derived ceramic composite coatings on steel. *J Eur Ceram Soc* 2008;**28**(1):253–7.
9. Nagaiah NR, Kapat JS, An L, Chow L. Novel polymer derived ceramic-high temperature heat flux sensor for gas turbine environment. *J Phys Conf Ser* 2006;**34**(1):458–63.
10. Ryu HY. Semiconductive behavior and the fabrication of a p–n junction diode from amorphous polymer-derived ceramics. PhD thesis, University of Colorado at Boulder; 2005.
11. Ferraioli L, Ahn D, Saha A, Pavesi L, Raj R. Intensely photoluminescent pseudo-amorphous siliconoxycarbonitride polymer–ceramic hybrids. *J Am Ceram Soc* 2008;**91**(July (7)):2422–4.
12. Zhang L, Wang Y, Wei Y, Xu W, Fang D, Zhai L, et al. A silicon carbonitride ceramic with anomalously high piezoresistivity. *J Am Ceram Soc* 2008;**9**(April (4)):1346–9.
13. Wang Y, Zhang L, Fan Y, Jiang D, An L. Stress-dependent piezoresis-tivity of tunneling-percolation systems. *J Mater Sci* 2009;**44**(June (11)): 2814–9.
14. Reddy SK, Cramer NB, Cross T, Raj R, Bowmen CN. Polymer-derived ceramic materials from thiol-ene photopolymerizations. *Chem Mater* 2003;**15**(November (22)):4257–61.
15. Schulz M, Borner M, Hausselt J, Heldele R. Polymer derived ceramic microparts from X-ray lithography—cross-linking behavior and process optimization. *J Eur Ceram Soc* 2005;**25**(2–3):199–204.
16. Friedel T, Travitzky N, Niebling F, Scheffler M, Greil P. Fabrication of polymer derived ceramic parts by selective laser curing. *J Eur Ceram Soc* 2005;**25**(2–3):193–7.
17. Liew LA, Zhang W, Bright VM, An L, Dunn ML, Raj R. Fabrication of SiCN ceramic MEMS using injectable polymer-precursor technique. *Sens Actuators A* 2001;**89**(1–2):64–70.
18. Cross T, Raj R. Mechanical and tribological behavior of polymer-derived ceramics constituted from SiC<sub>x</sub>O<sub>y</sub>N<sub>z</sub>. *J Am Ceram Soc* 2006;**89**(December (12)):3706–14.
19. Smith CS. Piezoresistance effect in germanium and silicon. *Phys Rev* 1954;**94**(1):42–9.
20. Toriyama T, Sugiyama S. Analysis of piezoresistance in *n*-type β-SiC for high-temperature mechanical sensors. *Appl Phys Lett* 2002;**81**(October (15)):2797–9.
21. Beheim G. Pressure sensors developed for high temperatures. *Aero Tech Innov* 2001;**9**(May/June (3)):16.
22. Korvink J, Paul O. *MEMS: a practical guide to design, analysis, and applications*. Norwich, NY: William Andrew Publishing; 2005.
23. Yamamoto A, Norio N, Takahiro T. *Diamond Relat Mater* 2007:1670.
24. *Diamond depositions: science and technology*. Superconductivity Publica-tions; 1995. p. 8–9.
25. Fahrner WR, Job R, Werner M. Sensors and smart electronics in harsh environment applications. *Microsyst Technol* 2001;**7**:138–44.